Journal of Materials Chemistry C

Accepted Manuscript

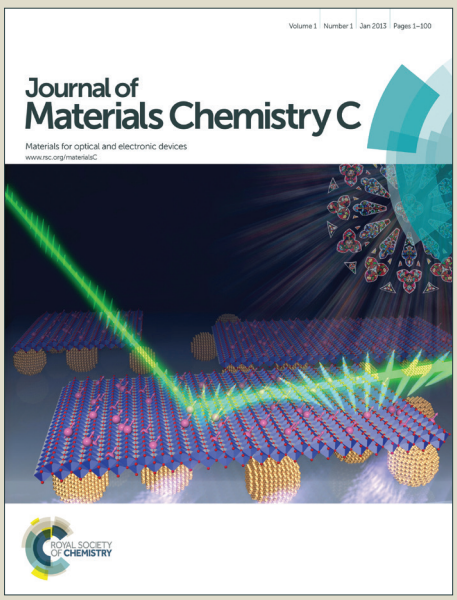

ROYAL SOCIETY OF CHEMISTRY

www.rsc.org/materialsC

Cite this: DOI: 10.1039/c0xx00000x

ARTICLE TYPE

www.rsc.org/xxxxxx

Structural Stability and Band Gap Tunability of Single-Side Hydrogenated Graphene from First-principles Calculations

Min Li, Lu Wang*, Ningning Yu, Xiaotian Sun, Tingjun Hou, Youyong Li*

Received (in XXX, XXX) Xth XXXXXXXXX 20XX, Accepted Xth XXXXXXXXX 20XX

DOI: 10.1039/b000000x

Based on density functional theory (DFT) calculations, we construct and investigate different types of single-side hydrogenated graphene (SSHG) structures from the structural motifs. Structural stability and electronic properties for these SSHG structures are extensively analyzed and compared with the reported structures. The single side hydrogenation makes a severe bending in graphene at a high H coverage, which makes the formation energy ascending with the increased H coverage. Among these SSHG structures that we have considered, the configurations with H attached along the armchair direction show the lowest formation energies due to a relatively small buckling compared to other configurations. Moreover, only the armchair hydrogenated graphene opens a band gap near the Fermi level, and the band gap can be modulated from zero to 1.44 eV as the H coverage varies from zero to 50%. Our results suggest an efficient way to prepare graphene-based materials and devices with suitable band gap.

1. Introduction

Graphene, a single-atomic layer of carbon atoms material, has unique properties over the other carbon allotropes. With the zero-gap electronic structure and the massless Dirac fermion behavior,[1,2] graphene has been considered as the most promising material in a wide range of fields.[3-7] However, lack of band gap limits its electronic applications greatly. Among the gap-opening strategies, chemical functionalization can efficiently transform the hybridization state of carbon atom from sp^2 into sp^3, which is recognized as the popular method to modify the electronic structure of graphene, such as functionalized by H, F, O and other species.[8-12] Among them, hydrogenation of graphene is a prototype case of covalent chemical functionalization. Fully hydrogenated graphene called "graphane" was first proposed theoretically by Sofo and co-workers,[13] which is an insulator with a direct band gap, and then successfully synthesized by exposing graphene in hydrogen plasma environment.[14] This reaction is reversible, making the hydrogen coverage flexible. Theoretical calculations have been performed by Zhao's group and they found that it is possible to continuously tune the band gap of hydrogenated graphene from 0 to 4.66 eV with the hydrogen coverage varying from 67 % to 100 %,[15] which enhanced its applications in semiconductor-based devices.

Till now, more studies have been focused on hydrogenated graphene with hydrogen on double sides,[15-18] but when the graphene is on a substrate surface, such as silicon oxide, the hydrogenation on both sides of graphene is impossible due to the difficult diffusion of hydrogen atoms along the graphene-substrate interface.[14,19] In experiments, the single-side hydrogenation of graphene was first observed by Elias et al. during their synthesis of graphane.[14] Later, Subrahmanyam et al. have also proved the existence of single-side hydrogenated graphene (SSHG) when they use the multilayer graphene for chemical hydrogen storage.[20] Besides, Balog et al. have demonstrated that the patterned hydrogen adsorption on graphene grown on Ir (111) surface can result in buckling ripples and open a band gap of 450 meV due to the Moiré superlattice of graphene and metal.[21] Theoretically, graphone with removing the hydrogen atoms from one side of graphane, was first proposed in 2009,[22] which is a ferromagnetic semiconductor with a small indirect gap of 0.46 eV. As the hydrogen atoms increase to full coverage on one side, it is still a semiconductor with a indirect band gap of 1.35 eV.[23] Although a series of investigations on SSHG have been performed,[22,24-26] these studies always focus on the configuration and energetic properties, lacking of the discussions on electronic properties, especially the relationship between the electronic structures and the H coverage on SSHG structures.

Here we systematically investigate the structural stability and electronic properties for SSHG by first-principles calculations. Starting from the hydrogen clusters (H_1-H_8) adsorbed on the graphene surface, we discuss several types of SSHG structures, including different shapes of hydrogen domain and H atoms attached along zigzag or armchair directions. Furthermore, the electronic properties for different types of SSHG with different H coverage are intensively studied. It is interesting to find that, the SSHG with hydrogen atom adsorbed along the armchair direction possesses the lowest formation energies, and only this kind of structure opens a moderate band gap, which can be continuously tuned from 0 to 1.44 eV with the H coverage from 0 to 50 %.

2. Computational Methods

Spin-polarized self-consistent field electronic structure calculations were performed with density-functional theory (DFT) implemented in DMol^3 code.[27,28] The exchange-correlation functional was treated by the generalized gradient approximation (GGA) with the PW91 parameterization.[29] All the structures were fully relaxed without any symmetry constraint. All-electron treatment and double numerical basis including *d*- and *p*-polarization function (DNP) were used.[27] A supercell (8×8 hexagonal unit cell) containing 128 carbon atoms was used to construct the hydrogenated graphene structures, and the supercell dimension for the direction perpendicular to the graphene sheet is chosen as 15 Å in order to avoid the interaction between neighboring graphene layers. The relaxation of atomic positions was considered to converge when the change of the total energy is less than 1.0×10^{-5} Ha/Å, the force on each atom is less than 0.002 Ha/Å, and the displacement is less than 0.005 Å.

To determine the stability of SSHG configurations, we define the formation energy per hydrogen by the following formula:

$$E_f = (E_{SSHG} - E_G - nE_H)/n \quad (1)$$

where E_{SSHG} and E_G are the total energies of the SSHG and the pristine graphene, respectively, and E_H is the total energy of an isolated H atom, n is the number of hydrogen atoms on graphene.

3. Results and Discussions

3.1 Hydrogen atoms (H_1-H_8) adsorbed on graphene by single side

In order to determine the stable SSHG structures, we search for low-energy zero-dimensional (0D) motifs, and then construct two-dimensional (2D) SSHG structures based on the 0D motifs. First, we search as much as possible geometric structures of hydrogen atoms (H_1-H_8) adsorbed on graphene by single side. For each motif, we have considered more than ten configurations and show two to six low-energy structures in Fig. 1 with the relative formation energy difference. When one hydrogen atom adsorbed on graphene, it prefers to locate at the top site of C atom with a C-H bond formed. The hydrogen atom makes the bonded C atom shift from the graphene plane and the shift height is 0.64 Å. The C-H bond length and the chemical adsorption energy for a H atom is 1.12 Å and 1.44 eV, respectively, which is close to the previous theoretical study. [17]

As shown in Fig. 1, from H_2 to H_8, all the configurations labeled as H_n^a possess the lowest formation energies, and the energy differences for the other configurations compared to H_n^a are also listed in the brackets. For instance, H_2^a configuration which includes two H in the neighboring site is the most stable configuration. The energy differences for the H_2^b and H_2^c configurations compared to H_2^a are 0.05 eV and 1.20 eV, respectively. For H_3 structures, there are four possible structures. The H_3^a configuration with three H atoms arranging at the neighboring sites in a hexagonal carbon ring has the same energy with H_3^b configuration. If the three H atoms locate at the alternating sites in a hexagonal carbon ring (H_3^d configuration), its formation energy will be 2.12 eV higher. For H_4 structures, six configurations have been considered. Four H atoms arranged at the neighboring sites like armchair pattern but in one hexagonal carbon ring (H_4^a configuration) shows the lowest formation energy. The formation energy of H_4^b configuration, combining two H_2^b configurations at the third neighbouring site, is comparable to that of H_4^a configuration. The energies of the other configurations are 0.11 eV, 0.38 eV, 1.50 eV and 1.78 eV higher for H_4^c, H_4^d, H_4^e and H_4^f structures, respectively. It is worthy to note that, from H_5 to H_8, the most stable configurations are all based on H_4^a configuration by adding more H atoms along the armchair direction. For H_6, there is also a H_6^b configuration has a low formation energy that a single benzenoid ring is isolated by three H_2^b motifs. The configuration of six H atoms bonded to six carbon atoms in the same carbon hexagonal ring is labeled as H_6^d, whose energy is 0.56 eV higher than H_6^a configuration. The most stable H_8^a configuration is the combination of two H_4^a motifs. It is easy to find that all the H^a structures share the same structural pattern or structural motif, that is, the hydrogen atoms prefer to adsorb on neighboring carbon atoms in order to maximize the number of sp^2 C-C bonds and the arrangement of these hydrogen atoms is along the armchair direction. Based on the stable structural motif, we construct different types of 2D SSHG configurations in the following discussions.

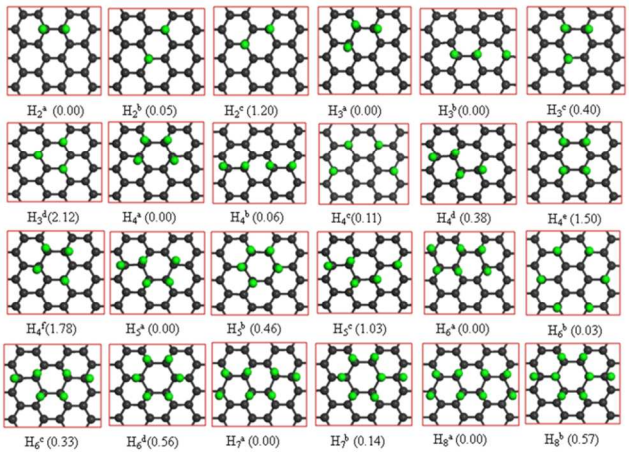

Fig.1 Optimized structures and the energy difference for H_2-H_8 adsorbed on the single side of graphene

Furthermore, we also consider the interactions between the motifs. We take the H_4^a motif as an example. It is found that two H_4^a motifs arranging along the armchair direction tend to bind to each other with the energy lowered by 0.77 eV. In comparison, combining two H_4^a motifs along the zigzag direction is not energetically favored. Thus, the armchair H chains are more stable than the corresponding zigzag chains, which is consistent with a previous study of oxygen adsorbed on graphene .[30]

3.2. Structural stability of SSHG with different H coverage

By using the 0D structural motifs described above as the building blocks, we investigate four kinds of SSHG structures: i) combining H_6^c motif to form a triangle H domain with zigzag H edge (Tri-H); ii) combining H_6^c motif to form a circle H domain with armchair H edge (Cir-H); iii) combining H_2^a motif to form a zigzag H chain (ZZ-H); iv) combining H_4^a motif to form a armchair H chain (AM-H). The structures are illustrated in Fig. 2a and the maximum H coverage considered here is 50%. Under optimization, transformation of the sp^2 C hybridization in pristine graphene to sp^3 C hybridization in SSHG structure results in a great change of bond lengths and bond angles, and all the

structures bend severely, especially for the structures with high H coverage.

Fig. 3 shows some representative structures of Cir-H with H coverage of 18.75% or 42.18% and AM-H with H coverage of 25% or 50%. The variation of C-H bond length and the shift height of hydrogenated C for these four types of SSHG with different H coverage are summarized in Table 1. For all these four types of SSHG structures, as the H coverage increases, the average C-H bond length slightly decreases and the shift height of hydrogenated C above the graphene plane increases significantly (as large as ~3.7 Å for the H coverage approaches to 50%). Compared to the other SSHG configurations, the AM-H shows a relatively small bending curvature (the shift height of hydrogenated C is less than 1.8 Å).

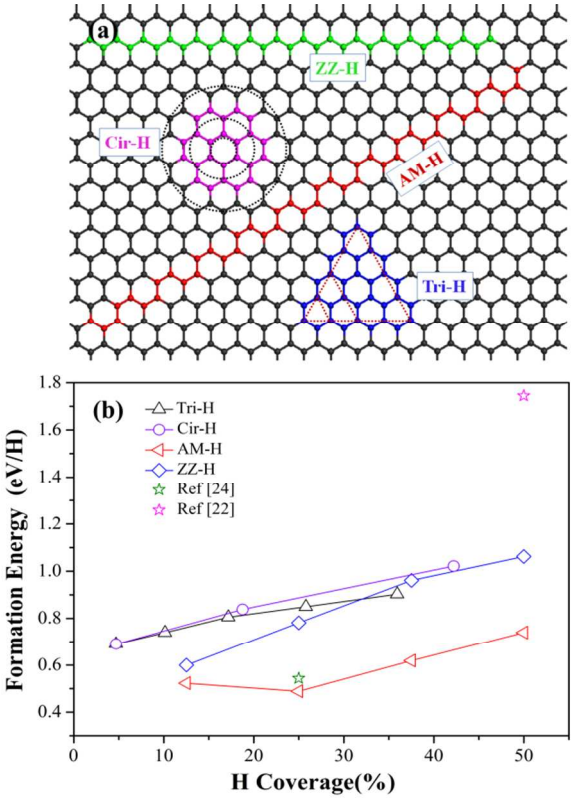

Fig.2 (a) Structural illustration for the four types of SSHG models (AM-H, Tri-H, ZZ-H, and Cir-H); (b) Formation energies per H for different SSHG structures as the function of H coverage. The hollow stars represent the formation energies of some structures reported in the previous literatures.[22, 24]

Table 1. Variation of C-H bond length and the shift height of hydrogenated C perpendicular to graphene plane for the four types of SSHG configurations (AM-H, ZZ-H, Cir-H, and Tri-H) with different H coverage.

system	AM-H				Cir-H			
H coverage (%)	12.5	25	37.5	50	4.7	18.8	42.2	--
C-H(Å)	1.111	1.106	1.104	1.102	1.103	1.092	1.089	--
Height(Å)	1.0	1.3	1.7	1.8	1.6	2.9	3.8	--
system	ZZ-H				Tri-H			
H coverage (%)	12.5	25	37.5	50	10.2	17.2	25.8	35.9
C-H(Å)	1.108	1.101	1.096	1.093	1.095	1.095	1.094	1.093
Height(Å)	1.6	2.2	2.8	3.3	2.4	2.9	3.1	3.5

To indentify the stability of the SSHG structures, we calculate the formation energies for these four types of structures with different H coverage and the results are shown in Fig. 2b. We find that the formation energy increases with the H coverage due to the increased strain energy, which is different from the hydrogenated graphene on both sides. [15] This can be explained by the competition between the strain energy induced by the bending and the gain in energy due to the formation of C-H bond. As shown in Fig. 3, when H coverage increases, the bending of the structures becomes more significant, so the stain energy plays an important role in the formation energy as the H coverage increases. It is also worthy to note that, all the formation energies for these structures are almost lower than 1.0 eV per H, which indicates the hydrogenation of graphene by single side is reversible, making the hydrogen coverage flexible.

For a given H coverage, the AM-H structure shows notably lower formation energy than the other three types of configurations, which indicate that the AM-H configurations are more energetically favorable. For instance, when H coverage is 25%, the formation energy for AM-H is 0.29 eV and 0.32 eV lower than that for ZZ-H and Tri-H, respectively. It is also comparable to the C_4H structure reported by Li et al. (the energy difference is only 0.022 eV at our computational level).[24] The AM-H structure with H coverage of 50% shows the formation energy of 0.74 eV, 0.32 eV and 1.01 eV lower than that for ZZ-H and graphone,[22] respectively. This can be explained by the contribution of the strain energy induced by the bending of graphene.

As shown in Table 1, the shift heights of hydrogenated C in the AM-H structures are 1.0-1.8 Å, but for the other three types of SSHG, the shift heights of hydrogenated C are as large as 3.7 Å at the H coverage of 50%. Therefore, the small bending curvature of AM-H structures leads to the low energy loss from strain effect, and finally results in low formation energy for AM-H structures. From Fig. 2b, the formation energy for AM-H with H coverage of 12.5% (the first dot in the red circle line) is slightly higher than that for AM-H with H coverage of 25%, that is because the corresponding AM-H structure is constructed by the H_2^b configuration (a half armchair H chain), whose energy is 0.05eV/H higher than that of the H_2^a configuration.

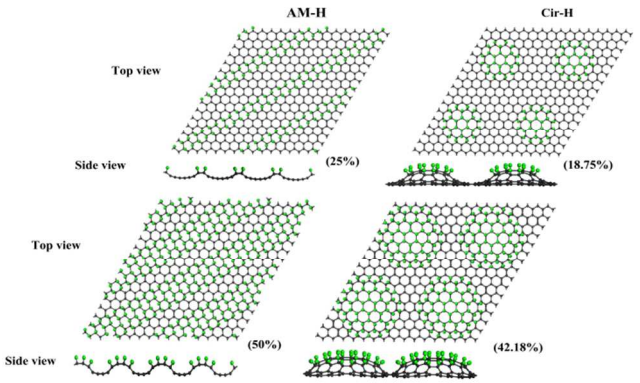

Fig.3 Top view and side view for AM-H and Cir-H structures with different H coverage.

3.3. Band gap tuning

Now we focus on the electronic properties for these four types of SSHG structures with different H coverage. Interestingly, we find that only the AM-H structure opens a band gap. In order to explain it, we analyze the local density of states (DOS) for these structures and the results are shown in Fig. 4. Our results reveal that at a given H coverage of 25%, the AM-H structure shows a small band gap of 0.52 eV, and the band gap increases to 1.44 eV at the H coverage of 50%. But for the other types of structures, there are always half-filled states at the Fermi level. As we dicussed above, the AM-H structures show the lowest formation energies, which can be attributed to this band-gap opening mechanism. Because the electronic properties have a close connection to the spatial arrangement of the sp^3 and sp^2 C distributions, we analyze the partial density of states for all the structures. The inset figure in Fig. 4b shows an example for AM-H structure with H coverage of 50%. As we know, C has two 2*s* and two 2*p* electrons, and hydrogen has 1*s* electron and no *p* electron. In hydrogenated graphene, the contributions around the Fermi level mainly comes from the *p* orbitals of the sp^2 C atoms. As H coverage increases, there are fewer sp^2 C atoms available for the formation of delocalized π bonds.

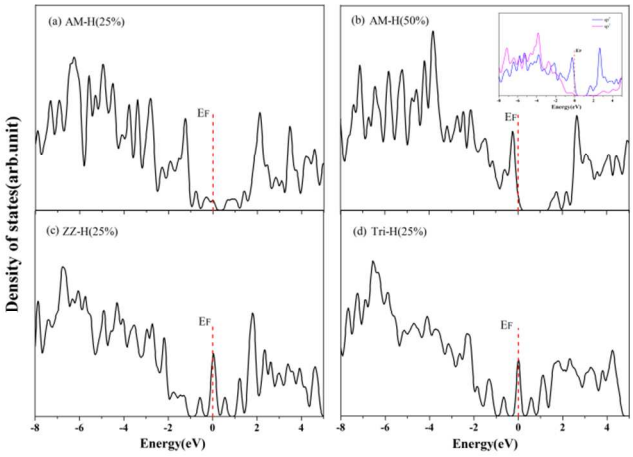

Fig.4 Density of states for AM-H structure with H coverage of (a) 25% and (b) 50%, (c) ZZ-H structure with H coverage of 25%, and (d) Tri-H structure with H coverage of 25%. The inset figure in (b) shows the partial density of states for sp^2 and sp^3 C atoms. Fermi level is set to zero as marked by the red dot line.

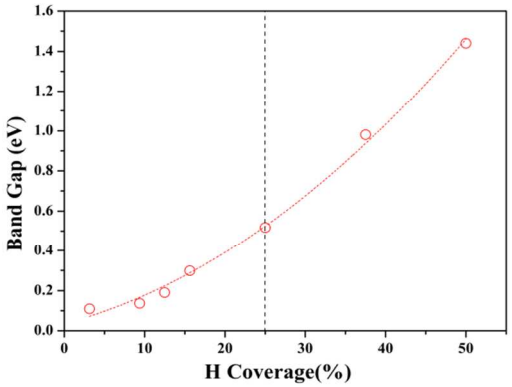

Fig. 5 Band gaps (eV) for AM-H structures as a function of H coverage (%).

We further investigate the band gap variation of the AM-H structures as a function of H coverage and the results are shown in Fig. 5. It is clearly seen that the band gap increases from 0 to 1.44 eV with H coverage from 0 to 50%. In this range, one can fit a third polynomial relationship for the band gap (y in eV) of the AM-H strucure versus the H coverage (x in %) as:

$$y=0.03514+0.0106x+0.00035816x^2 \quad (2)$$

A previous theoretical report has shown that the GGA computation may underestimate the band gap by ~13.7% with regard to the more accurate GW method.[15] Thus the gaps of these hydrogenated graphene systems might slightly higher than the values reported here.

When the H coverage changes from 0 to 25%, the AM-H structure is constructed by connecting more H_4^a motif along the AM direction, and eventually form an AM H chain at the H coverage of 25%. The band gap increases from 0.1 eV for one H_4^a motif adsorbed on graphene to 0.52 eV for forming a AM H chain. Then, we enlarge the width of the AM H chain with H coverage varies from 25% to 50%. The band gap can be tuned from 0.52 eV to 1.44eV. Compared to the graphone with a band gap of 0.46 eV [22] and the insulator of C_4H structure with a band gap of 3.43 eV, [24] our proposed SSHG structures show a tunable band gap between visible light and near-infrared regions (ca. 0.5-1.5 eV). This may lead to potential applications in electronics and photonics.

4. Conclusions

We carry out a systematic study on structural and electronic properties for SSHG structures by first-principles calculations. We reveal that the H clusters prefer to aggregate along the armchair direction to form armchair H chain. For a given H coverage, the AM-H structure is the most stable compared to the other types of structures, which can be explained by the relatively small bending of AM-H structures and the relatively small strain energy loss. Our analysis of electronic properties shows that, only the AM-H configuration opens a band gap, and the band gap can be tuned from 0.52 eV to 1.44 eV by enlarging the width of the AM H chain with increasing H coverage. The unique structural and electronic properties make the SSHG structures promising for applications in electronic and photonic devices.

Acknowledgement

The work is supported by the National Basic Research Program of China (973 Program, Grant No. 2012CB932400), the National Natural Science Foundation of China (Grant No. 21403146, 91233115, 21273158 and 91227201), Natural Science Foundation of Jiangsu Province (Grant No. BK20140314), a Project Funded by the Priority Academic Program Development of Jiangsu Higher Education Institutions (PAPD). This is also a project supported by the Fund for Innovative Research Teams of Jiangsu Higher Education Institutions, Jiangsu Key Laboratory for Carbon-Based Functional Materials and Devices, Collaborative Innovation Center of Suzhou Nano Science and Technology.

Notes and references

Functional Nano & Soft Materials Laboratory (FUNSOM) and Collaborative Innovation Center of Suzhou Nano Science and Technology

Jiangsu Key Laboratory for Carbon-Based Functional Materials & Devices, Soochow University, Suzhou, Jiangsu 215123, China. E-mail:lwang22@suda.edu.cn (Dr. Lu Wang); yyli@suda.edu.cn (Prof. Youyong Li)

1. K. Novoselov, A. K. Geim, S. Morozov, D. Jiang, M. Katsnelson, I. Grigorieva, S. Dubonos and A. Firsov, *Nature*, 2005, **438**, 197-200.
2. K. Nomura and A. MacDonald, *Phys. Rev. Lett.*, 2007, **98**, 076602.
3. A. A. Balandin, S. Ghosh, W. Bao, I. Calizo, D. Teweldebrhan, F. Miao and C. N. Lau, *Nano Lett.*, 2008, **8**, 902-907.
4. C. Lee, X. Wei, J. W. Kysar and J. Hone, *Science*, 2008, **321**, 385-388.
5. S. Gilje, S. Han, M. Wang, K. L. Wang and R. B. Kaner, *Nano Lett.*, 2007, **7**, 3394-3398.
6. A. K. Geim, *Science*, 2009, **324**, 1530-1534.
7. F. Bonaccorso, Z. Sun, T. Hasan and A. Ferrari, *Nat. Photonics*, 2010, **4**, 611-622.
8. D.W.Boukhvalov and M. I. Katsnelson, *J. Phys-Condens. Mat.*, 2009, **21**, 344205.
9. D. W. Boukhvalov, *Nanotechnology*, 2011, **22**, 055708.
10. Q. Tang, Z. Zhou and Z. Chen, *Nanoscale*, 2013, **5**, 4541-4583.
11. D. W. Boukhvalov and M. I. Katsnelson, *Phys. Rev. B*, 2008, **78**, 085413.
12. V. Georgakilas, M. Otyepka, A. B. Bourlinos, V. Chandra, N. Kim, K. C. Kemp, P. Hobza, R. Zboril and K. S. Kim, *Chem. Rev.*, 2012, **112**, 6156-6214.
13. J. O. Sofo, A. S. Chaudhari and G. D. Barber, *Phys. Rev. B*, 2007, **75**, 153401.
14. D. C. Elias, R. R. Nair, T. M. G. Mohiuddin, S. V. Morozov, P. Blake, M. P. Halsall, A. C. Ferrari, D. W. Boukhvalov, M. I. Katsnelson, A. K. Geim and K. S. Novoselov, *Science*, 2009, **323**, 610-613.
15. H. Gao, L. Wang, J. Zhao, F. Ding and J. Lu, *J. Phys. Chem. C*, 2011, **115**, 3236-3242.
16. M. Z. S. Flores, P. A. S. Autreto, S. B. Legoas and D. S. Galvao, *Nanotechnology*, 2009, **20**, 465704.
17. D. W. Boukhvalov, M. I. Katsnelson and A. I. Lichtenstein, *Phys. Rev. B*, 2008, **77**, 035427.
18. P. Chandrachud, B. S. Pujari, S. Haldar, B. Sanyal and D. Kanhere, *J. Phys-Condens. Mat.*, 2010, **22**, 465502.
19. J. S. Bunch, S. S. Verbridge, J. S. Alden, A. M. van der Zande, J. M. Parpia, H. G. Craighead and P. L. McEuen, *Nano Lett.*, 2008, **8**, 2458-2462.
20. K. Subrahmanyam, P. Kumar, U. Maitra, A. Govindaraj, K. Hembram, U. V. Waghmare and C. N. R. Rao, *Proc. Nat. Acad. Sci.*, 2011, **108**, 2674-2677.
21. R. Balog, B. Jorgensen, L. Nilsson, M. Andersen, E. Rienks, M. Bianchi, M. Fanetti, E. Laegsgaard, A. Baraldi, S. Lizzit, Z. Sljivancanin, F. Besenbacher, B. Hammer, T. G. Pedersen, P. Hofmann and L. Hornekaer, *Nat. Mater.*, 2010, **9**, 315-319.
22. J. Zhou, Q. Wang, Q. Sun, X. S. Chen, Y. Kawazoe and P. Jena, *Nano Lett.*, 2009, **9**, 3867-3870.
23. B. S. Pujari, S. Gusarov, M. Brett and A. Kovalenko, *Phys. Rev. B*, 2011, **84**, 041402.
24. Y. Li and Z. Chen, *J. Phys. Chem. C*, 2012, **116**, 4526-4534.
25. H. J. Xiang, E. J. Kan, S.-H. Wei, X. G. Gong and M. H. Whangbo, *Phys. Rev. B*, 2010, **82**, 165425.
26. L. Feng and W. X. Zhang, *AIP Adv.*, 2012, **2**, 042138.
27. B. Delley, *CA Chem. Phys.*, 1990, **92**, 508.
28. B. Delley, *J. Chem. Phys.*, 2000, **113**, 7756.
29. J. P. Perdew and Y. Wang, *Phys. Rev. B*, 1992, **45**, 13244.
30. L. Wang, Y. Sun, K. Lee, D. West, Z. Chen, J. Zhao and S. Zhang, *Phys. Rev. B*, 2010, **82**, 161406..

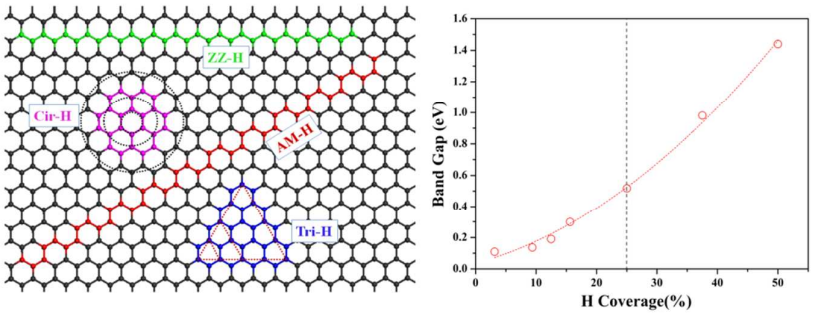

Hydrogenation of graphene on single side can efficiently tune the band gap between visible light and near-infrared regions.